Preprint of the paper:

"A massively parallel BEM numerical model for grounding analysis in layered soils"

I. Colominas, J. Gómez-Calviño, F. Navarrina, M. Casteleiro (2001)
En "II European Conference on Computational Mechanics: Solids, Structures and Coupled Problems in Engineering" (en CD-ROM), Parte VIII:
"High-Performance Computing in Mechanics"(21 páginas). Z. Waszczyszyn, J. Pamin (Editors); Institute of Computer Methods in Civil Engineering, Cracow University of Technology, Cracovia, Polonia. (ISBN: 83-85688-68-4)

http:/caminos.udc.es/gmni

ECCM-2001

European Conference on
Computational Mechanics

June 26-29, 2001
Cracow, Poland

A MASSIVELY PARALLEL BEM NUMERICAL MODEL FOR GROUNDING ANALYSIS IN LAYERED SOILS

Ignasi Colominas, Javier Gómez-Calviño and Fermín Navarrina

Department of Applied Mathematics
Civil Engineering School. Universidad de La Coruña, La Coruña, Spain
e-mail: colominas@iccp.udc.es

Manuel Casteleiro

Department of Mechanical Engineering
Northwestern University, Evanston, USA
e-mail: m-casteleiro@northwestern.edu

Key words: Grounding, Multilayer soil models, Parallelization

Abstract. *In the last years the authors have developed a numerical formulation based on the Boundary Element Method for the analysis of grounding systems embedded in uniform soils. This approach has been implemented in a CAD system that currently allows to analyze real grounding grids in real-time in personal computers.*
In this paper we present a numerical approach based on the boundary element method for grounding analysis in stratified soils which is a generalization of the previous one. The computational requirements for these models are noticeable higher, but the proposed formulation has been implemented in a high-performance parallel computer and the code has been applied to the analysis of several real grounding systems. We focus our attention in horizontally and vertically two layered soils and we discuss the results obtained in the application of the proposed method to some practical examples.

1 Introduction

One of the challenging problems stated from the beginnings of the industrial use of electricity is obtaining the potential distribution in large electrical installations when a fault current is derived into the soil through a grounding system. The main element of a grounding system of an electrical installation is strictly speaking the grounding grid or the "grounded electrode", being the potential distribution on the earth surface the most important parameter that it is necessary to know in order to design a safe grounding system.

In practice, in most of the large electrical instalations, the grounding grid usually consists of a mesh of interconnected cylindrical conductors, horizontally buried and supplemented by ground rods vertically thrusted in certain places of the substation site. Thus, its main objective is the transport and dissipation of electrical currents produced during fault conditions into the ground, ensuring that a person in the vicinity of the grounded installation is not exposed to a critical electrical shock, and preserving the continuity of the power supply and the integrity of the equipment. To attain these goals, the apparent electrical resistance of the grounding system must be low enough to guarantee that fault currents dissipate mainly through the grounding electrode into the soil. Moreover, electrical potential values between close points on the earth surface that can be connected by a person must be kept under certain maximum safe limits (step, touch and mesh voltages)[1,2].

In the last four decades, several methods and procedures for the analysis and design of grounding grids have been proposed. Most of these methods are generally based on the professional experience, on semi-empirical works, on experimental data obtained from scale model assays and laboratory tests, or on intuitive ideas. Undoubtedly, these contributions represented an important improvement in the grounding analysis area. However, some problems have been established and reported such as the large computational costs required in the analysis of real cases, unrealistic results obtained when segmentation of conductors is increased, and uncertainty in the margin of error[1,3].

Maxwell's Electromagnetic Theory is the starting point to derive the equations that govern the dissipations of electrical currents into a soil. Nevertheless, although these equations are well-known for years, their application and resolution for the computing of grounding grids of large installations in practical cases present serious difficulties. First, it is obvious that no analytical solutions can be obtained for most of real problems. On the other hand, the characteristic geometry of grounding systems (a mesh of interconnected bare conductors with a relatively small ratio diameter-length) makes very difficult the use of numerical methods. Thus, the use of some widespread numerical techniques commonly applied for solving boundary value problems in engineering, such as finite elements or finite differences, is extremely costly since it is required the discretization of the domain: the ground excluding the electrode. Consequently, obtaining sufficiently accurate results should imply unacceptable computing efforts in memory storage and CPU time.

In the last years, the authors have developed a numerical formulation based on the Boundary Element Method for the analysis of grounding systems with uniform soil models[4,5]. This approach has been implemented in a CAD application for earthing systems[6,7] that allows to analyze real grounding installations in real-time using personal computers. Recently, we have presented a generalization of the boundary element formulation for grounding grids embedded in layered soils[8]. In this paper, we present a summary of this general BE approach, we analyze the parallelization of the numerical formulation, and its application to several practical cases by using the geometry of a real grounding grid.

2 Equations of the Mathematical Model of the Problem

2.1 General Equations

Governing equations of the dissipation of electrical currents into the soil through a grounded electrode can be deduced from Maxwell's electromagnetic equations. Thus, if we restrict the analysis to obtaining the electrokinetic steady-state response and neglect the inner resistivity of the grounding conductors (then, potential can be assumed constant at every point of the grounding electrode surface), the 3D problem can be written as

$$\begin{aligned} &\mathrm{div}(\boldsymbol{\sigma}) = 0, \quad \boldsymbol{\sigma} = -\boldsymbol{\gamma}\,\mathbf{grad}(V) \text{ in } E\ ; \\ &\boldsymbol{\sigma}^t \boldsymbol{n}_E = 0 \text{ in } \Gamma_E\ ; \quad V = V_\Gamma \text{ in } \Gamma\ ; V \to 0, \text{ if } |\boldsymbol{x}| \to \infty; \end{aligned} \tag{1}$$

where E is the earth, $\boldsymbol{\gamma}$ is its conductivity tensor, Γ_E is the earth surface, $\boldsymbol{n}_E$ is its normal exterior unit field and Γ is the electrode surface[5].

Therefore, the solution to problem (1) gives the potential V and the current density $\boldsymbol{\sigma}$ at an arbitrary point $\boldsymbol{x}$, when the grounded electrode attains a voltage V_Γ (Ground Potential Rise, or GPR) relative to remote earth. Then, from (1) it is possible to obtain the potential distribution on the earth surface (and consequently, the step, mesh and touch voltages of the grounding system), as much as the total surge current and the equivalent resistance of the grounding grid by means of the current density $\boldsymbol{\sigma}$ on Γ[1,2]. On the other hand, from here on, it will be used the normalized boundary condition $V_\Gamma = 1$, since V and $\boldsymbol{\sigma}$ are proportional to the GPR value[5].

The most commonly soil model considered in many of the methods proposed for grounding analysis is the homogeneous and isotropic one, being conductivity $\boldsymbol{\gamma}$ substituted by an apparent scalar conductivity γ that must be experimentally obtained[1]. Clearly, this hypothesis does not introduce significant errors if the soil is "essentially uniform" in all directions in the vicinity of the grounding grid[1], and this model can also be used with loss of accuracy if the soil resistivity changes slightly with depth. Nevertheless, safety parameters involved in the grounding design can strongly vary if the soil electrical properties change through the substation site. These variations can be due to changes in the material nature, or in the humidity of the soil, for example.

For this reason, it is necessary to develop more advanced models to consider variations of the soil conductivity in the surroundings of the grounding site. Obviously, taking into account all variations of soil conductivity would be meaningless and unaffordable, neither from the economical nor from the technical point of view. For this reason, more practical soil models have been proposed. A family of these soil models consists of assuming the soil stratified in a number of horizontal or vertical layers, defined by an appropriate thickness and an apparent scalar conductivity that must be experimentally obtained. In fact, it is widely accepted that two-layer soil models should be sufficient to obtain good and safe designs of grounding systems in most practical cases[1]. This paper is devoted to studying the application of numerical methods for grounding analysis in layered soil models, specially in cases with two different horizontal or vertical layers (figures 1 and 2).

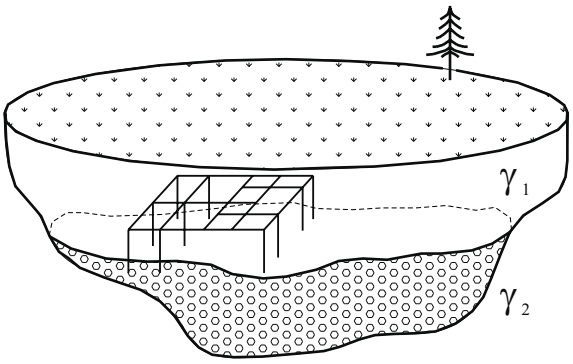

Fig. 1. Scheme of a soil model with two horizontal layers.

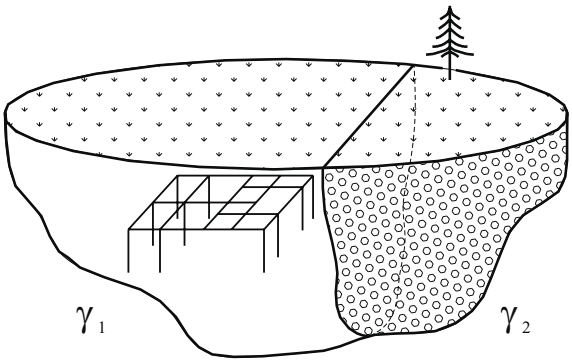

Fig. 2. Scheme of a soil model with two vertical layers.

In the hypothesis of a stratified soil model formed by C layers with different conductivities, the mathematical problem (1) can be written in terms of the following Neumann exterior problem[8]

$$\begin{aligned} &\mathrm{div}(\boldsymbol{\sigma}_c) = 0,\ \boldsymbol{\sigma}_c = -\gamma_c\,\mathbf{grad}(V_c) \text{ in } E_c,\ 1 \leq c \leq C; \\ &\boldsymbol{\sigma}_1^t \boldsymbol{n}_E = 0 \text{ in } \Gamma_E,\ V_b = 1 \text{ in } \Gamma; \\ &V_c \to 0 \text{ if } |\boldsymbol{x}| \to \infty,\ \boldsymbol{\sigma}_c^t \boldsymbol{n}_c = \boldsymbol{\sigma}_{c+1}^t \boldsymbol{n}_c \text{ in } \Gamma_c,\ 1 \leq c \leq C-1; \end{aligned} \tag{2}$$

where b denotes the layer in which the grounded electrode is buried, E_c is each one of the soil layers, γ_c is its scalar conductivity, V_c is the potential at an arbitrary point in the layer E_c, $\boldsymbol{\sigma}_c$ is its corresponding current density, Γ_c is the interface between layers E_c and E_{c+1}, and $\boldsymbol{n}_c$ is the normal field to Γ_c[8].

2.2 Integral Expression for Potential V and Variational Form of the Problem

As we have exposed in the introductory part, most of grounding grids of real electrical substations consist of a mesh of interconnected bare cylindrical conductors, horizontally buried and supplemented by ground rods. The ratio between the diameter and the length of the conductors uses to be relatively small ($\sim 10^{-3}$). This apparently simple geometry implies serious troubles in the modellization of the problem. In most of real cases, neither analytical solutions can be obtained, nor widespread numerical methods (such as FEM or FDM) can be used since the required discretization of the 3D domains E_c (excluding the grounding electrode) should involve a completely out of range computing effort. For these reasons, we have turned our attention to other numerical techniques which require only the discretization of the boundaries. With this aim, it is firstly essential to derive an integral expression for potential V in terms of unknowns defined on the boundary[5].

The deduction of this integral expression for the potential can be performed if we introduce in the model one fact related with the engineering problem, that is, the levelling and regularization processes of the surroundings of the substation site during the construction process of the electrical installation. Thus, the earth surface Γ_E and the interfaces Γ_c between layers can be assumed horizontal; consequently we will adopt an "horizontally layered soil model" in our mathematical model in order to catch the variations of the soil conductivity with depth (figure 1). In the case of variations of the soil conductivity near the grounding system, the simplest model we can state (a "vertically layered soil model") consist of asuming that the earth surface Γ_E is horizontal, while the interfaces Γ_c are parallel one to another and perpendicular to Γ_E (figure 2).

With these new assumptions, the application of the "method of images" and Green's Identity to problem (2) yields the following integral expression[8] for potential $V_c(\boldsymbol{x}_c)$ at an arbitrary point $\boldsymbol{x}_c \in E_c$, in terms of the unknown leakage current density $\sigma(\boldsymbol{\xi})$ ($\sigma = \boldsymbol{\sigma}^t \boldsymbol{n}$, where $\boldsymbol{n}$ is the normal exterior unit field to Γ) at any point $\boldsymbol{\xi}$ of the electrode surface $\Gamma \subset E_b$:

$$V_c(\boldsymbol{x_c}) = \frac{1}{4\pi\gamma_b} \int \int_{\boldsymbol{\xi}\in\Gamma} k_{bc}(\boldsymbol{x}_c, \boldsymbol{\xi})\, \sigma(\boldsymbol{\xi}) d\Gamma, \ \forall \boldsymbol{x}_c \in E_c, \tag{3}$$

where integral kernels $k_{bc}(\boldsymbol{x}_c, \boldsymbol{\xi})$ are formed by series of infinite terms corresponding to the resultant images obtained when Neumann exterior problem (2) is transformed into a Dirichlet one[8,9]. Depending on the type of the soil model, these series can have an infinite or a finite number of terms. In the case of uniform soil ($C = 1$), they are reduced to only two summands since there is only one image of the original grid[4,5]:

$$k_{11}(\boldsymbol{x}_1, \boldsymbol{\xi}) = \frac{1}{r(\boldsymbol{x}_1, [\xi_x, \xi_y, \xi_z])} + \frac{1}{r(\boldsymbol{x}_1, [\xi_x, \xi_y, -\xi_z])}, \tag{4}$$

where $r(\boldsymbol{x}_1, [\xi_x, \xi_y, \xi_z])$ indicates the distance from $\boldsymbol{x}_1$ to $\boldsymbol{\xi} \equiv [\xi_x, \xi_y, \xi_z]$, being the point $[\xi_x, \xi_y, -\xi_z]$ the symmetric one of $\boldsymbol{\xi}$ with respect to the earth surface Γ_E. We assume

that the origin of the coordinates system is on the earth surface and the z-axis is perpendicular to Γ_E.

If we consider the case of a vertical two-layered model (figure 2), the series of the kernels are also reduced to a finite number of terms:

$$\begin{aligned} k_{11}(\boldsymbol{x}_1, \boldsymbol{\xi}) = & \frac{1}{r(\boldsymbol{x}_1, [\xi_x, \xi_y, \xi_z])} + \frac{1}{r(\boldsymbol{x}_1, [\xi_x, \xi_y, -\xi_z])} \\ & + \frac{\kappa}{r(\boldsymbol{x}_1, [\xi_x, -\xi_y, \xi_z])} + \frac{\kappa}{r(\boldsymbol{x}_1, [\xi_x, -\xi_y, -\xi_z])} \end{aligned} \tag{5}$$

$$k_{12}(\boldsymbol{x}_2, \boldsymbol{\xi}) = \frac{1+\kappa}{r(\boldsymbol{x}_2, [\xi_x, \xi_y, \xi_z])} + \frac{1+\kappa}{r(\boldsymbol{x}_2, [\xi_x, \xi_y, -\xi_z])}$$

where $r(\boldsymbol{x}, [\xi_x, \xi_y, \xi_z])$ indicates the distance from $\boldsymbol{x}$ to $\boldsymbol{\xi}$. The other terms correspond to the distances from $\boldsymbol{x}$ to the symmetric point of $\boldsymbol{\xi}$ with respect to the earth surface Γ_E, and to the resultant images with respect to the vertical interface. We assume again that the origin of the coordinates system is on the earth surface and on the vertical interface, and the z-axis and y-axis are perpendicular to Γ_E and Γ_1 respectively. Ratio κ is defined in terms of the layer conductivities

$$\kappa = \frac{\gamma_1 - \gamma_2}{\gamma_1 + \gamma_2}. \tag{6}$$

In the case of an horizontal two-layered soil model (figure 1), the expressions of the integral kernels are given by

$$\begin{aligned} k_{11}(\boldsymbol{x}_1, \boldsymbol{\xi}) = & \sum_{i=0}^{\infty} \frac{\kappa^i}{r(\boldsymbol{x}_1, [\xi_x, \xi_y, 2iH + \xi_z])} + \sum_{i=0}^{\infty} \frac{\kappa^i}{r(\boldsymbol{x}_1, [\xi_x, \xi_y, 2iH - \xi_z])} \\ & + \sum_{i=1}^{\infty} \frac{\kappa^i}{r(\boldsymbol{x}_1, [\xi_x, \xi_y, -2iH + \xi_z])} + \sum_{i=1}^{\infty} \frac{\kappa^i}{r(\boldsymbol{x}_1, [\xi_x, \xi_y, -2iH - \xi_z])}; \\ k_{12}(\boldsymbol{x}_2, \boldsymbol{\xi}) = & \sum_{i=0}^{\infty} \frac{(1+\kappa)\kappa^i}{r(\boldsymbol{x}_2, [\xi_x, \xi_y, -2iH + \xi_z])} + \sum_{i=0}^{\infty} \frac{(1+\kappa)\kappa^i}{r(\boldsymbol{x}_2, [\xi_x, \xi_y, -2iH - \xi_z])}; \\ k_{21}(\boldsymbol{x}_1, \boldsymbol{\xi}) = & \sum_{i=0}^{\infty} \frac{(1-\kappa)\kappa^i}{r(\boldsymbol{x}_1, [\xi_x, \xi_y, -2iH + \xi_z])} + \sum_{i=0}^{\infty} \frac{(1-\kappa)\kappa^i}{r(\boldsymbol{x}_1, [\xi_x, \xi_y, 2iH - \xi_z])}; \\ k_{22}(\boldsymbol{x}_2, \boldsymbol{\xi}) = & \frac{1}{r(\boldsymbol{x}_2, [\xi_x, \xi_y, \xi_z])} - \frac{\kappa}{r(\boldsymbol{x}_2, [\xi_x, \xi_y, 2H + \xi_z])} + \sum_{i=0}^{\infty} \frac{(1-\kappa^2)\kappa^i}{r(\boldsymbol{x}_2, [\xi_x, \xi_y, -2iH + \xi_z])}; \end{aligned} \tag{7}$$

In the above expressions, $r(\boldsymbol{x}, [\xi_x, \xi_y, \xi_z])$ indicates the distance from $\boldsymbol{x}$ to $\boldsymbol{\xi}$. The other terms correspond to the distances from $\boldsymbol{x}$ to the symmetric point of $\boldsymbol{\xi}$ with respect to

the earth surface Γ_E, and to the interface surface between layers. H is the thickness of the upper layer, and κ is given by (6). We assume once more that the origin of the coordinates system is on the earth surface and the z-axis is perpendicular to Γ_E.

Another type of soil model that it can be derived from the soil model with two vertical layers is given in figure 3. This soil model would correspond to a common situation in practical cases of electrical substations located near urban zones when the vertical interphase is a retaining wall.

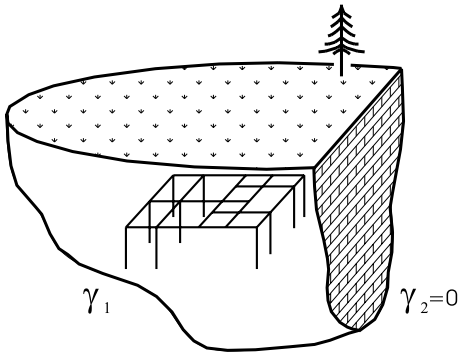

Fig. 3. Scheme of a soil model when the vertical interphase is a retaining wall.

For this soil model, the weakly singular kernel is a particular case of (5) when $\kappa = 0$ and then

$$\begin{aligned} k_{11}(\boldsymbol{x}_1, \boldsymbol{\xi}) = & \frac{1}{r(\boldsymbol{x}_1, [\xi_x, \xi_y, \xi_z])} + \frac{1}{r(\boldsymbol{x}_1, [\xi_x, \xi_y, -\xi_z])} \\ & + \frac{1}{r(\boldsymbol{x}_1, [\xi_x, -\xi_y, \xi_z])} + \frac{1}{r(\boldsymbol{x}_1, [\xi_x, -\xi_y, -\xi_z])} \end{aligned} \tag{8}$$

where $r(\boldsymbol{x}, [\xi_x, \xi_y, \xi_z])$ indicates the distance from $\boldsymbol{x}$ to $\boldsymbol{\xi}$. The rest of the terms correspond to the distances from $\boldsymbol{x}$ to the symmetric point of $\boldsymbol{\xi}$ with respect to the earth surface Γ_E, and to the resultant images with respect to the vertical interface (the origin of the coordinates system is on the earth surface and on the vertical interface, and the z-axis and y-axis are perpendicular to Γ_E and Γ_1 respectively). In this soil model, it is meaningless to compute the potential $V_2(\boldsymbol{x_2})$, and therefore the kernel $k_{12}(\boldsymbol{x}_2, \boldsymbol{\xi})$ is not used.

From expressions (4), (5), (7) and (8), it is clear that singular kernels $k_{bc}(\boldsymbol{x}_c, \boldsymbol{\xi})$ for uniform and two-layer soil models can be written in a general form

$$k_{bc}(\boldsymbol{x}_c, \boldsymbol{\xi}) = \sum_{l=0}^{l_k} k_{bc}^l(\boldsymbol{x}_c, \boldsymbol{\xi}), \quad k_{bc}^l(\boldsymbol{x}_c, \boldsymbol{\xi}) = \frac{\psi^l(\kappa)}{r(\boldsymbol{x}_c, \boldsymbol{\xi}^l(\boldsymbol{\xi}))}, \tag{9}$$

where ψ^l is a weighting coefficient that depends only on the ratio κ given by (6), and $r(\boldsymbol{x}_c, \boldsymbol{\xi}^l(\boldsymbol{\xi}))$ is the Euclidean distance between the points $\boldsymbol{x}_c$ and $\boldsymbol{\xi}^l$, being $\boldsymbol{\xi}^0$ the point $\boldsymbol{\xi}$

on the electrode surface ($\boldsymbol{\xi}^0(\boldsymbol{\xi}) = \boldsymbol{\xi}$), and being $\boldsymbol{\xi}^l$ ($l \neq 0$) the images of $\boldsymbol{\xi}$ with respect to the earth surface and to the interfaces between layers[8,9]. Finally, l_k is the number of summands in the series of integral kernels, and it depends on the case being analyzed (see (4), (5), (7) and (8)).

Expression (3) is very important for the solution of the problem since it allows to obtain the value of the electrical potential at an arbitrary point $\boldsymbol{x}_c$ if the leakage current density σ is known. Furthermore, it is also possible to compute the total surge current that flows from the grounding system, its equivalent resistance and most of the remaining safety and design parameters of a grounding grid[5]. The leakage current density σ can be obtained by solving the following Fredholm integral equation of the first kind on Γ

$$\frac{1}{4\pi\gamma_b} \iint_{\boldsymbol{\xi}\in\Gamma} k_{bb}(\boldsymbol{\chi},\boldsymbol{\xi})\sigma(\boldsymbol{\xi})\, d\Gamma = 1, \qquad \forall \boldsymbol{\chi} \in \Gamma. \tag{10}$$

since the integral expression for the potential (3) is also satisfied on the electrode surface Γ, where the potential value is known by the boundary condition $V_b(\boldsymbol{\chi}) = 1$, $\forall \boldsymbol{\chi} \in \Gamma$. Now, we can obtain a variational form of this integral expression imposing that it is verified in the sense of weighted residuals, that is, the following integral identity

$$\iint_{\boldsymbol{\chi}\in\Gamma} w(\boldsymbol{\chi}) \left(\frac{1}{4\pi\gamma_b} \iint_{\boldsymbol{\xi}\in\Gamma} k_{bb}(\boldsymbol{\chi},\boldsymbol{\xi})\sigma(\boldsymbol{\xi})\, d\Gamma - 1 \right) d\Gamma = 0, \tag{11}$$

must hold for all members $w(\boldsymbol{\chi})$ of a suitable class of test functions defined on Γ[4,5]. It is important to remark that the solution of equation (10) only requires obtaining the leakage current density σ in points of the electrode surface (and no in points of the 3D domain). Consequently, a numerical method based on the discretization of the boundaries of the domain, such as the Boundary Element Method[5,10], should be the best numerical approach for solving it.

3 BEM Numerical Formulation

3.1 General 2D approach

The starting point of the development of a numerical approach based on the BEM is the discretization of the unknown leakage current density σ and the electrode surface Γ, in terms of a given set of $\mathcal{N}$ trial functions $\{N_i(\boldsymbol{\xi})\}$ defined on Γ and a given set of $\mathcal{M}$ 2D boundary elements $\{\Gamma^\alpha\}$:

$$\sigma(\boldsymbol{\xi}) = \sum_{i=1}^{\mathcal{N}} \sigma_i\, N_i(\boldsymbol{\xi}), \qquad \Gamma = \bigcup_{\alpha=1}^{\mathcal{M}} \Gamma^\alpha, \tag{12}$$

Now, it is possible to discretize the integral expression (3) for the potential $V_c(\boldsymbol{x}_c)$:

$$V_c(\boldsymbol{x}_c) = \sum_{i=1}^{\mathcal{N}} \sigma_i V_{c,i}(\boldsymbol{x}_c); \;\; V_{c,i}(\boldsymbol{x}_c) = \sum_{\alpha=1}^{\mathcal{M}} \sum_{l=0}^{l_V} V_{c,i}^{\alpha l}(\boldsymbol{x}_c); \tag{13}$$

$$V_{c,i}^{\alpha l}(\boldsymbol{x}_c) = \frac{1}{4\pi\gamma_b} \iint_{\boldsymbol{\xi}\in\Gamma^\alpha} k_{bc}^l(\boldsymbol{x}_c, \boldsymbol{\xi})\, N_i(\boldsymbol{\xi})\; d\Gamma^\alpha; \tag{14}$$

where l_V represents the number of summands to consider in the evaluation of the series of kernels until convergence is achieved ($l_V = l_k$ if this number is finite).

Finally, the variational form (11) is reduced to the following linear system of equations for a given set of $\mathcal{N}$ test functions $\{w_j(\boldsymbol{\chi})\}$ defined on Γ:

$$\begin{gathered} \sum_{i=1}^{\mathcal{N}} R_{ji}\sigma_i = \nu_j \qquad (j = 1, \ldots, \mathcal{N}) \\ R_{ji} = \sum_{\beta=1}^{\mathcal{M}} \sum_{\alpha=1}^{\mathcal{M}} \sum_{l=0}^{l_R} R_{ji}^{\beta\alpha l}, \qquad \nu_j = \sum_{\beta=1}^{\mathcal{M}} \nu_j^\beta, \end{gathered} \tag{15}$$

being

$$R_{ji}^{\beta\alpha l} = \frac{1}{4\pi\gamma_b} \iint_{\boldsymbol{\chi}\in\Gamma^\beta} w_j(\boldsymbol{\chi}) \iint_{\boldsymbol{\xi}\in\Gamma^\alpha} k_{bb}^l(\boldsymbol{\chi}, \boldsymbol{\xi}) N_i(\boldsymbol{\xi}) d\Gamma^\alpha d\Gamma^\beta, \tag{16}$$

$$\nu_j^\beta = \iint_{\boldsymbol{\chi}\in\Gamma^\beta} w_j(\boldsymbol{\chi}) d\Gamma^\beta, \tag{17}$$

where l_R represents the number of summands to consider in the evaluation of the series of kernels until convergence is achieved ($l_R = l_k$ if this number is finite).

Solution of the linear system (14) provides the values of the current densities σ_i ($i = 1, \ldots, \mathcal{N}$) leaking from the nodes of the grid. However, In practice, the 2D discretization required to solve the above stated equations in real problems implies an extremely large number of degrees of freedom. In addition, the coefficient matrix in (15) is full and the computation of each contribution (16) requires double integration on a 2D domain[5] and, in the case of kernels given by infinite series, an extremely high number of evaluations of terms of the kernel. For these reasons, it is essential to introduce some additional simplifications in the BEM approach to decrease the computational cost.

3.2 Approximated 1D BE approach

With this aim, and taking into account the real geometry of grounding grids in most of electrical substations, one can assume that the leakage current density is constant around the cross section of the cylindrical electrode[5]. This hypothesis of "circumferential uniformity" is widely used in most of the theoretical developments and practical procedures proposed for grounding analysis[1].

Consequently, if we denote L the whole set of axial lines of the buried conductors, $\widehat{\boldsymbol{\xi}}$ the orthogonal projection over the bar axis of a given generic point $\boldsymbol{\xi} \in \Gamma$, $\phi(\widehat{\boldsymbol{\xi}})$ the electrode diameter, $P(\widehat{\boldsymbol{\xi}})$ the circumferential perimeter of the cross section in $\widehat{\boldsymbol{\xi}}$, and

$\widehat{\sigma}(\widehat{\boldsymbol{\xi}})$ the approximated leakage current density at this point (assumed uniform around the cross section), we can derive an approximated expression for potential (3) as,

$$\widehat{V}_c(\boldsymbol{x}_c) = \frac{1}{4\gamma_b} \int_{\widehat{\boldsymbol{\xi}} \in L} \phi(\widehat{\boldsymbol{\xi}})\, \bar{k}_{bc}(\boldsymbol{x}_c, \widehat{\boldsymbol{\xi}})\, \widehat{\sigma}(\widehat{\boldsymbol{\xi}})\; dL, \quad \forall \boldsymbol{x}_c \in E_c \tag{18}$$

being $\bar{k}_{bc}(\boldsymbol{x}_c, \widehat{\boldsymbol{\xi}})$ the average of the integral kernel $k_{bc}(\boldsymbol{x}_c, \widehat{\boldsymbol{\xi}})$ in the cross section in $\widehat{\boldsymbol{\xi}}$:

$$\bar{k}_{bc}(\boldsymbol{x}_c, \widehat{\boldsymbol{\xi}}) = \int_{\boldsymbol{\xi} \in P(\widehat{\boldsymbol{\xi}})} k_{bc}(\boldsymbol{x}_c, \boldsymbol{\xi}) dP. \tag{19}$$

Now, the variational identity (11) will not hold, because the leakage current is not exactly uniform around the cross section and boundary condition $V_1(\boldsymbol{\chi}) = 1$, $\boldsymbol{\chi} \in \Gamma$ will not be strictly satisfied at every point $\boldsymbol{\chi}$ on Γ. For it, restricting the class of trial functions to those with circumferential uniformity (i.e., $w(\boldsymbol{\chi}) = \widehat{w}(\widehat{\boldsymbol{\chi}})\ \forall \boldsymbol{\chi} \in P(\widehat{\boldsymbol{\chi}})$), we obtain the new variational form

$$\frac{1}{4\gamma_b} \int_{\widehat{\boldsymbol{\chi}} \in L} \phi(\widehat{\boldsymbol{\chi}})\, \widehat{w}(\widehat{\boldsymbol{\chi}}) \left[\int_{\widehat{\boldsymbol{\xi}} \in L} \phi(\widehat{\boldsymbol{\xi}})\, \bar{\bar{k}}_{bb}(\widehat{\boldsymbol{\chi}}, \widehat{\boldsymbol{\xi}})\, \widehat{\sigma}(\widehat{\boldsymbol{\xi}})\, dL \right] dL = \int_{\widehat{\boldsymbol{\chi}} \in L} \phi(\widehat{\boldsymbol{\chi}})\, \widehat{w}(\widehat{\boldsymbol{\chi}})\, dL, \tag{20}$$

which it must be verify for all functions $\widehat{w}(\widehat{\boldsymbol{\chi}})$ of a suitable class of test ones defined on L, where integral kernel $\bar{\bar{k}}_{bb}(\widehat{\boldsymbol{\chi}}, \widehat{\boldsymbol{\xi}})$ is given by

$$\bar{\bar{k}}_{bb}(\widehat{\boldsymbol{\chi}}, \widehat{\boldsymbol{\xi}}) = \int_{\boldsymbol{\chi} \in P(\widehat{\boldsymbol{\chi}})} \left[\int_{\boldsymbol{\xi} \in P(\widehat{\boldsymbol{\xi}})} k_{bb}(\boldsymbol{\chi}, \boldsymbol{\xi})\, dP \right] dP. \tag{21}$$

In contrast to integral equation (11), the resolution of (20) requires the discretization of the whole set of axial lines L of the grounded conductors. Thus, the unknown approximated leakage current density $\widehat{\sigma}$ and the axial lines L can be discretized if we consider a set of n trial functions $\{\widehat{N}_i(\widehat{\boldsymbol{\xi}})\}$ defined on L, and a set of m 1D boundary elements $\{L^\alpha\}$:

$$\widehat{\sigma}(\widehat{\boldsymbol{\xi}}) = \sum_{i=1}^{n} \widehat{\sigma}_i\, \widehat{N}_i(\widehat{\boldsymbol{\xi}}), \qquad L = \bigcup_{\alpha=1}^{m} L^\alpha, \tag{22}$$

Now, it is possible to discretize the approximated potential (18)

$$\widehat{V}_c(\boldsymbol{x}_c) = \sum_{i=1}^{n} \widehat{\sigma}_i\, \widehat{V}_{c,i}(\boldsymbol{x}_c); \qquad \widehat{V}_{c,i}(\boldsymbol{x}_c) = \sum_{\alpha=1}^{m} \sum_{l=0}^{l_V} \widehat{V}_{c,i}^{\alpha l}(\boldsymbol{x}_c); \tag{23}$$

$$\widehat{V}_{c,i}^{\alpha l}(\boldsymbol{x}_c) = \frac{1}{4\gamma_b} \int_{\widehat{\boldsymbol{\xi}} \in L^\alpha} \phi(\widehat{\boldsymbol{\xi}})\, \bar{k}_{bc}^{l}(\boldsymbol{x}_c, \widehat{\boldsymbol{\xi}})\, \widehat{N}_i(\widehat{\boldsymbol{\xi}})\; dL^\alpha, \tag{24}$$

where l_V represents the number of summands to consider in the evaluation of the series of kernels until convergence is achieved ($l_V = l_k$ if this number is finite).

Finally, the variational form (20) is also reduced to a linear system of equations for a given set of n test functions $\{\widehat{w}_j(\widehat{\boldsymbol{\chi}})\}$ defined on L:

$$\begin{gathered} \sum_{i=1}^{n} \widehat{R}_{ji}\widehat{\sigma}_i = \widehat{\nu}_j \qquad (j=1,\ldots,n) \\ \widehat{R}_{ji} = \sum_{\beta=1}^{m}\sum_{\alpha=1}^{m}\sum_{l=0}^{l_R} \widehat{R}_{ji}^{\beta\alpha l}, \qquad \widehat{\nu}_j = \sum_{\beta=1}^{m} \widehat{\nu}_j^{\beta}, \end{gathered} \tag{25}$$

where

$$\widehat{R}_{ji}^{\beta\alpha l} = \frac{1}{4\gamma_b} \int_{\widehat{\boldsymbol{\chi}}\in L^\beta} \phi(\widehat{\boldsymbol{\chi}})\, \widehat{w}_j(\widehat{\boldsymbol{\chi}}) \int_{\widehat{\boldsymbol{\xi}}\in L^\alpha} \phi(\widehat{\boldsymbol{\xi}})\, \overline{\overline{k}}_{bb}^{\,l}(\widehat{\boldsymbol{\chi}},\widehat{\boldsymbol{\xi}})\, \widehat{N}_i(\widehat{\boldsymbol{\xi}})\, dL^\alpha dL^\beta, \tag{26}$$

$$\widehat{\nu}_j^{\beta} = \int_{\widehat{\boldsymbol{\chi}}\in L^\beta} \phi(\widehat{\boldsymbol{\chi}})\, \widehat{w}_j(\widehat{\boldsymbol{\chi}})\, dL^\beta. \tag{27}$$

In contrast with the 2D boundary element general formulation, the number of elemental contributions needed to state the system of linear equations (25) and the number of unknowns σ_i are now significantly smaller for a given level of mesh refinement. In spite of the important reduction in the computational cost, extensive computing is still necessary mainly because of the circumferential integration on the perimeter of the electrodes that are involved in the integral kernels. In previous works we have proposed the approximated evaluation of these circumferential integrals by using specific quadratures[5]. The final result is an approximated 1D formulation in which the coefficients of the equations system only requires integration on 1D domains, i.e. the axial lines of the electrodes[8].

Different choices of the sets of trial and test functions allow to derive specific numerical approaches[5]. In this paper, we have selected a Galerkin type one, where the matrix of coefficients is symmetric and positive definite[10]. On the other hand, the authors have derived a highly efficient analytical technique to evaluate the coefficients of the linear system of equations[5] for Point Collocation and Galerkin type weighting in uniform soil models. Since the 1D approximated expressions for the terms $\widehat{V}_{c,i}^{\alpha l}$ and $\widehat{R}_{ji}^{\beta\alpha l}$ in (24) and (26) are formally equivalent to those obtained in the case of uniform soil models, their computation can also be performed analytically by menas of the above mentioned techniques[5,8].

In next sections we present some examples of this numerical formulation applied to the grounding analysis by considering different type of soil models. We discuss its total computational cost, its implementation and the need of parallelization of the programming codes.

4 Examples of application of the proposed BEM formulation

4.1 Grounding grid and soil models studied

In this section a complete application example of the Boundary Element numerical formulation will be presented. The numerical approach proposed up to here has been implemented in a Computer Aided Design system[6]. This tool performs grounding analysis for all the soil models exposed in the previous sections.

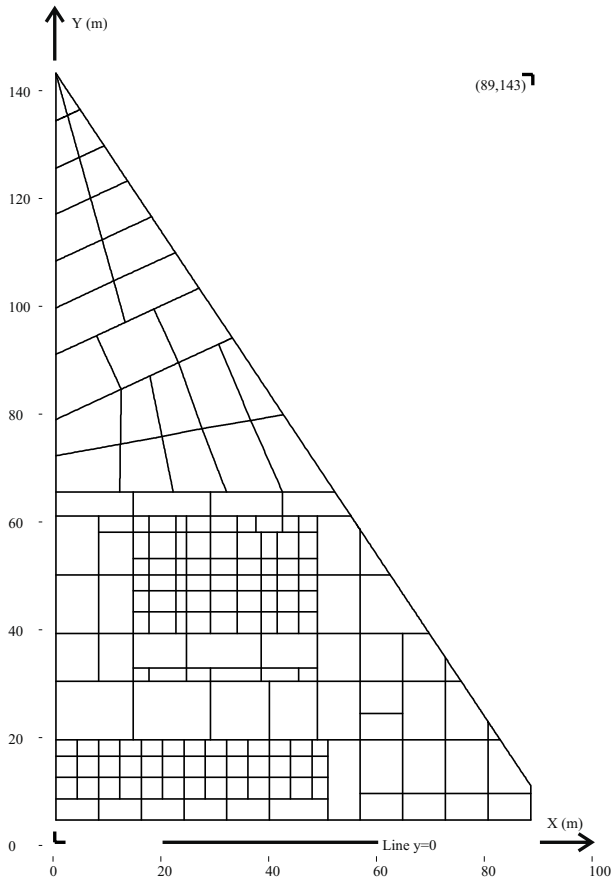

Fig. 4. Barberá grounding system: Plan of the grid buried to a depth of 0.8 m.

The example consists of the application of the CAD system to the analysis of the large real earthing grid of the Barberá substation, near the city of Barcelona in Spain. This earthing system is formed by a grid of 408 segments of cylindrical conductor of the same diameter (12.85 mm) buried to a depth of 80 cm. The grounding system has a right-angled triangle shape of 143×89 m^2 and protects a total area of 6,600 m^2. The grid has been discretized in 408 linear leakage current elements which implies 238 degrees of freedom. The Ground Potential Rise (GPR) considered in this study has

been 10 kV. The plan of the grounding grid and its dimensions are shown in figure 4. This grounding system has been calculated by using the following soil models:

Model A is an homogeneous soil model with conductivity $\gamma = 0.016\,(\Omega m)^{-1}$, corresponding to the case of an uniform terrain made, for example, of clay.

Model B is a vertically layered soil (see figure 2), being the conductivity of the part of the soil that contains the earthing grid $\gamma_1 = 0.016\,(\Omega m)^{-1}$, and the other side $\gamma_2 = 0.005\,(\Omega m)^{-1}$ representing a less conductive soil.

Model C is similar to model B but with $\gamma_2 = 0\,(\Omega m)^{-1}$; this corresponds to the case of taking into account the presence of a retaining wall for example (see figure 3), quite frequent in substations placed into urban areas.

Model D is an horizontally layered soil (see figure 1), being $\gamma_1 = 0.005\,(\Omega m)^{-1}$ the conductivity of the upper layer, $\gamma_2 = 0.016\,(\Omega m)^{-1}$ the conductivity of the lower layer, and $h = 1\ m$ the thickness of the upper layer.

4.2 Results of application of the numerical formulation

The Barberá grounding grid has been computed by using the numerical model proposed in section 3 with the four soil models, and the results of these calculations will be represented from now on in several ways. The equivalent resistance, the total surge current of the grounding system computed in each case are summarized in Table I.

TABLE I. Barberá grounding system: Numerical results by using different soil models.

Soil Model	**Eq. Resistance** (Ω)	**Total Current** (kA)	**CPU Time** (s)
A	0.3128	31.97	9.7
B	0.3712	26.94	18.4
C	0.4163	24.02	18.3
D	0.3705	26.99	1724.2

In figure 5 we can see the potential distribution on the earth surface obtained for each one of the four cases. The differences between the results are noticeable, mainly near the $Y = 0$ line (models B and C) and in the general potential levels (model D).

Figure 6 shows a detail of the potential distribution in the surroundings of the south-eastern corner of the earthing grid. In the soil model B we can notice how electrical current (perpendicular to the isopotential lines represented) suffers refraction when passing through the vertical boundary between different soils (plane Y = 0). In the soil model C (vertical retaining wall in $Y = 0$ line) it can be seen that electrical current is parallel to the wall surface (isopotential lines perpendicular to that surface), as expected.

With a color scale, figure 7 shows the potential distribution in the vertical plane $Y = 0$ for soil models C (the surface is the wall itself) and soil model D. Potentials shown for soil model C may be specially useful when studying touch voltage for the wall surface. In the soil model D a change in the potential evolution with depth must be noticed when trespassing the $Z = -1m$ level.

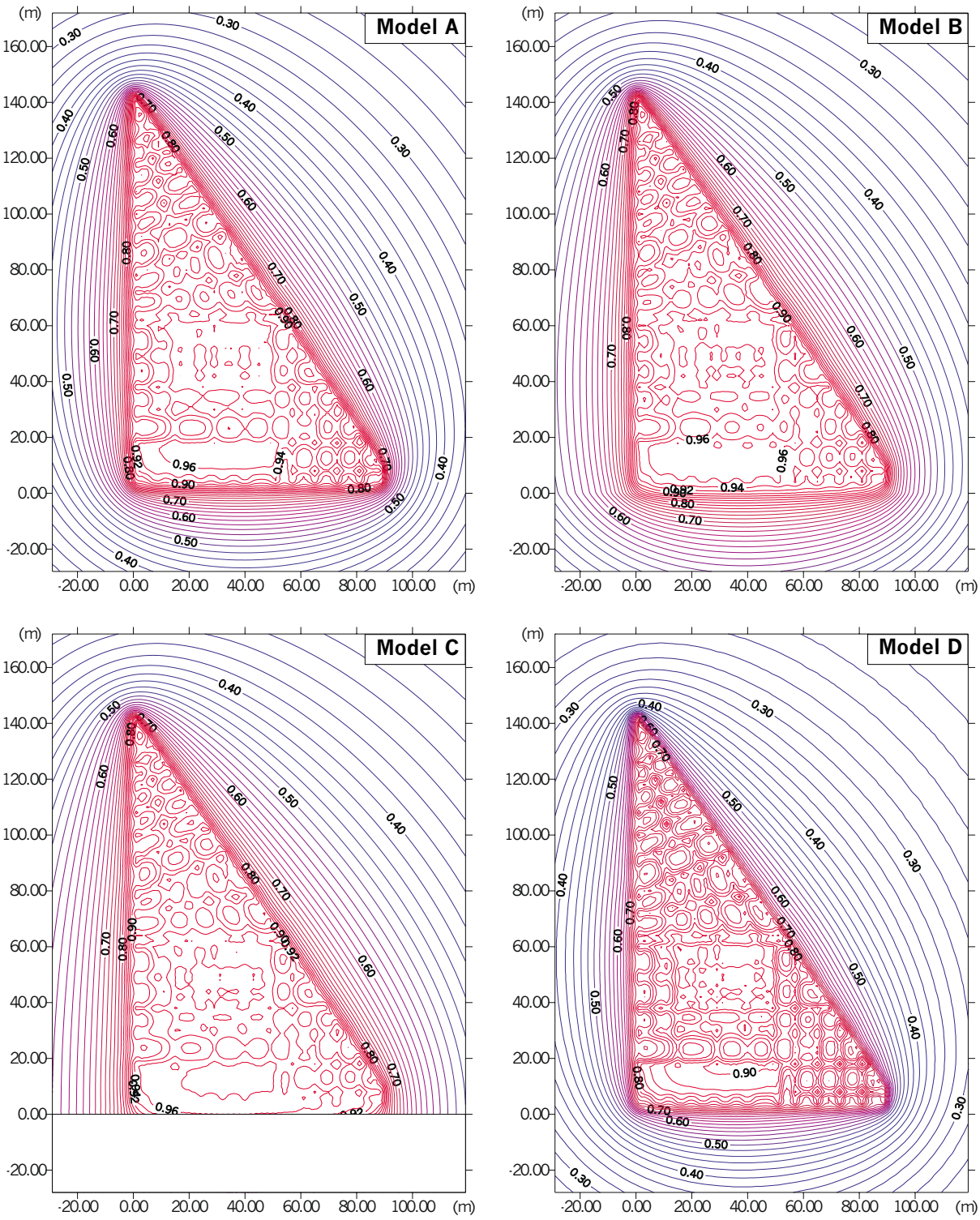

Fig. 5. Potential levels on the earth surface for soil models A (uniform soil), B (two vertical layers), C (vertical retaining wall), and D (two horizontal layers). At the scale of the figure it is very difficult to notice, but in soil model C isopotential lines are perpendicular to the wall interphase as expected.

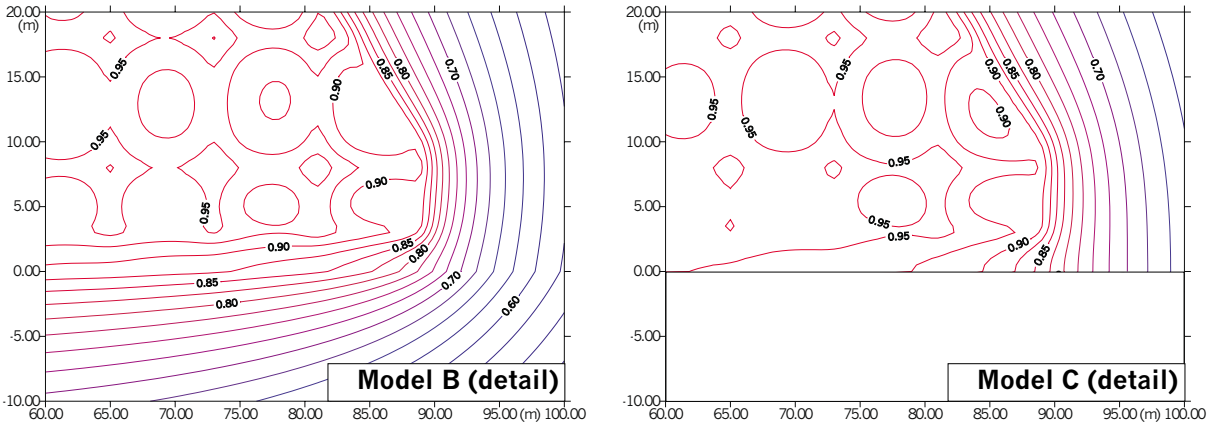

Fig. 6. Potential levels on the earth surface, detail of SE corner of the grounding grid, for the soil models B and C

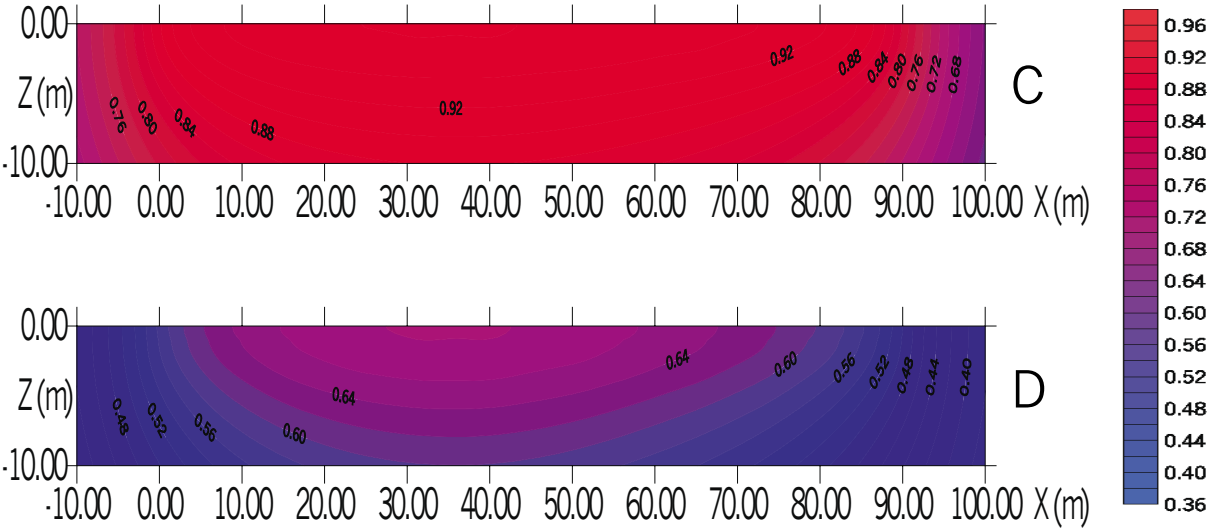

Fig. 7. Potential levels in plane $Y = 0$ for the soil models C (vertical retaining wall in $Y = 0$) and D (two horizontal layers)

Figure 8 shows potential levels for the models studied along two different lines onto the earth surface: line $X = 6$, and line $Y = 13$. Model D potentials are considerably lower than the other ones because the grid is embebbed in a quite more resistive surface soil. In the top picture we can see that potential levels A, B, C are quite similar far from the vertical boundary but ones get different from the other ones when the point is near that boundary (near point $Y = 0$).

As expected, the results obtained can strongly depend on the soil model used in the grounding analysis. Two-layer models can get more accurate results than employing a uniform soil model. Therefore, it could be advisable to use multi-layer soil formulations to analyze grounding systems as a general rule, in spite of the increase of the compu-

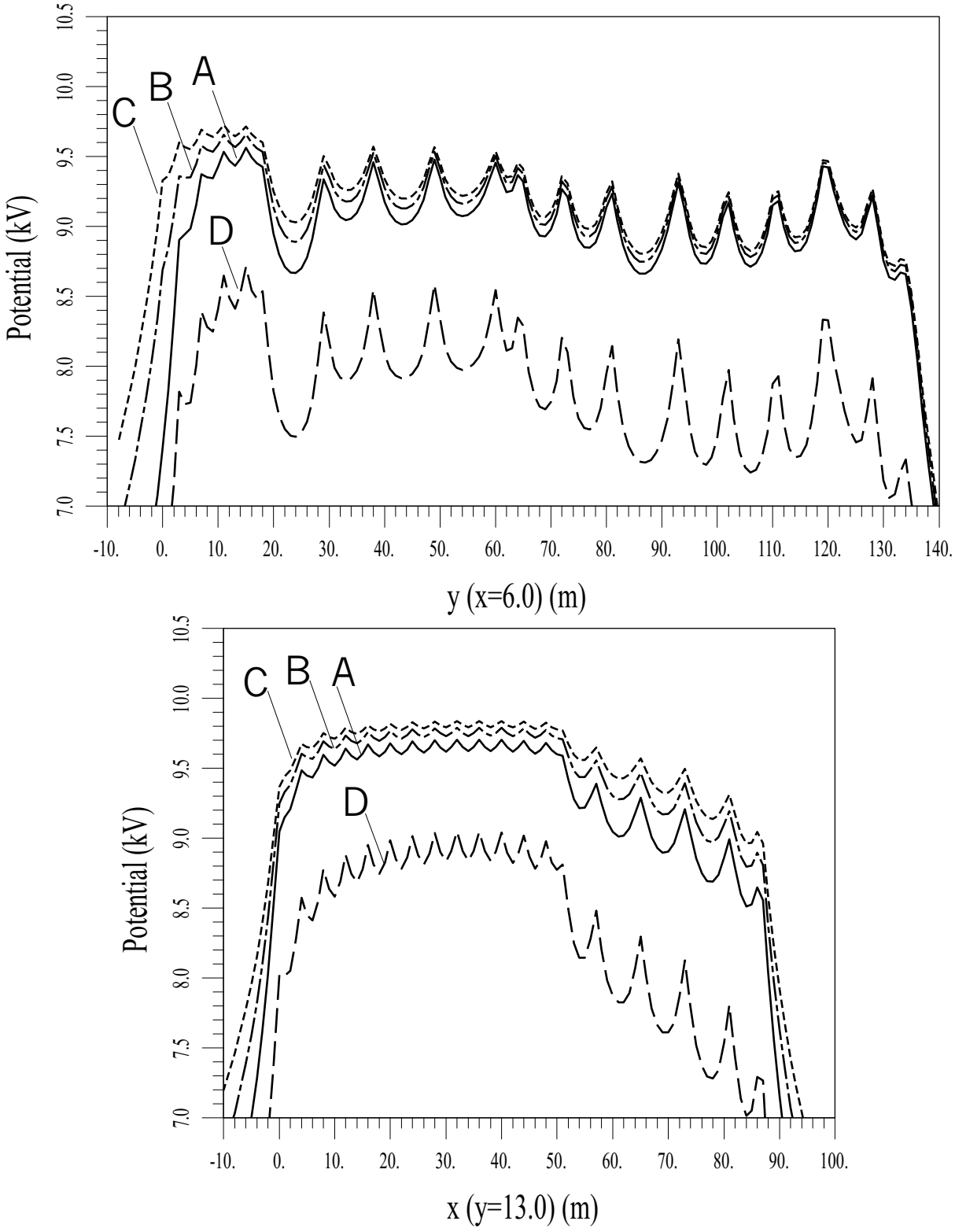

Fig. 8. Potential levels (with GPR=10kV) along surface line x=6 and surface line y=13

tational effort. In fact, the use of this kind of advanced models should be mandatory in cases where the conductivity of the soil changes markedly with depth. Soil model D has shown how a different resistivity in a thin surface soil layer can affect considerably to the potential distribution obtained.

Nevertheless, as we can see in the CPU time of Table I, while single-layer models (and in general soil models with integral kernels with a finite number of terms) run in real time in conventional computers for the analysis of medium/big size grounding grids, multiple-layer models non-vertical boundaries (like model D) require in general an out of order computing time (basically, because it is necessary to compute a high number of terms of the infinite series of the integral kernels). For this reason, we have studied the parallelization of the horizontal layer model BEM numerical approach, so that it could become a real-time design tool for grounding analysis.

5 Parallelization of the proposed BEM formulation

5.1 Objective algorithms to parallelize

The computational cost that the proposed formulation implies is as follows, for specific discretization (m elements of p nodes each, and a total number of n degrees of freedom). A linear system (25) of order n must be generated and solved.

The system matrix generation process requires $O(n^2p^2/2)$ operations, since p^2 series of contributions of type (26) have to be computed for every pair of elements, and approximately half of them are discarded because of symmetry. In uniform soil models these series are formed by only two terms and in vertically layered soil models they will be formed by four terms. But in two horizontal layers models the series have an infinite number of them, that will be numerically added up until a tolerance is fulfilled or an upper limit of summands is achieved. Consequently, matrix generation will be much more expensive in horizontal layer models (like soil model D in the previous section).

The linear system solving process requires $O(n^3/3)$ operations (since the matrix is symmetric but not sparse) if the resolution is carried out with a direct method. This would be unaffordable in large problems, so the semiiterative technique of the diagonal preconditioned conjugate gradient algorithm with assembly of the global matrix has been implemented. This technique results extremely efficient for solving large scale problems, with a very low computational cost in comparison with matrix generation. So the cost of the system resolution should never prevail.

On the other hand, once the leakage current has been obtained, the cost of computing the equivalent resistance is negligible. The additional cost of computing potential at any given point (normally at the earth surface) by means of only requires $O(mp)$ operations, since p series of contributions of type (24) have to be computed for every element. However, if it is necessary to compute potentials at a large number of points (i.e. to draw contours), computing time may be important.

So the most critical time-consuming process of this numerical formulation based on the Boundary Element Method is matrix generation, followed by computation of potential at a large number of points once the leakage current density has been obtained. Since both processes accept massive parallelization, computing time could be reduced under acceptable levels, even for cases of extremely large models, if the number of available processors is high enough, in spite of the efficiency loses due to the data transfer overhead and the system administration workload.

In this section we will discuss the parallelization (that is, the distribution of different tasks of the program among several processors) of the matrix generation process, applying it to the numerical code corresponding to the horizontal layer model BEM numerical formulation[11].

For confirming the computational cost predictions made above, the computing times of every part of the leakage current density process (before calculation of potentials) have been measured during the sequential computation of an horizontally layered soil model. The result is very significant: 99.94% of the total computing time (1724.21 seconds) is devoted to matrix generation.

5.2 Parallel computer and parallelization mode

The numerical approach has been implemented on a CAD system, which has been compiled and run onto an *Origin 2000 Silicon Graphics* computer at the *European Center for Parallelism of Barcelona* (CEPBA). The compilation process of the code has been made in sequential and parallel modes, and the executions have been run for the uniform and the two-layer models. The CPU time required for each soil model case can be found in Table I.

The O2000 used in our work is a high-performance computer with 64 MIPS R10000 processors at 250 MHz. It has a peak performance of 32 GFlops. Internally, the O2000 is organised in clusters of 2 processors sharing a main memory of 256 Mbyte. Each processor has 4 Mbyte of cache memory. The clusters are connected by an hypercube network. Each processor can access all the distributed main memory through the network. Then, the O2000 can be programmed as an 8 Gbyte shared memory machine. The input/output devices have a capability of 1.2 Gbytes/s.

The parallelization mode selected for this problem has been the use of compiler directives, following the present OpenMP standard. This selection is justified because: *a)* a shared memory computer is available for running the program (necessary condition for using compiler parallelization directives), *b)* the use of compiler directives grants clearness to a parallel code that may be handled in the future, *c)* the OpenMP syntax assures the portability of the parallel code to any shared memory computer, and *d)*, as we will see below, the loop to be run in parallel is transformable into an adequate form so that directives are efficient.

5.3 Parallelization of the code

Equation (25) shows that the matrix generation process is performed by means of a double loop that couples every element with all the other ones ($m(m+1)/2$ cycles). Into each cycle, the elemental matrix corresponding to a pair of elements is calculated and immediately assembled into the system matrix. If we try to parallelize this double loop, we find that the assembly of the elemental matrices causes a dependency between the actions of the threads or processes. This drawback can be avoided by taking the assembly process out of that loop, which implies first the computation and the storage of all the elemental matrices and, after this step, the assembly in a sequential mode. This scheme requires approximately twice memory space than the original one, but in any case this memory space is not very large.

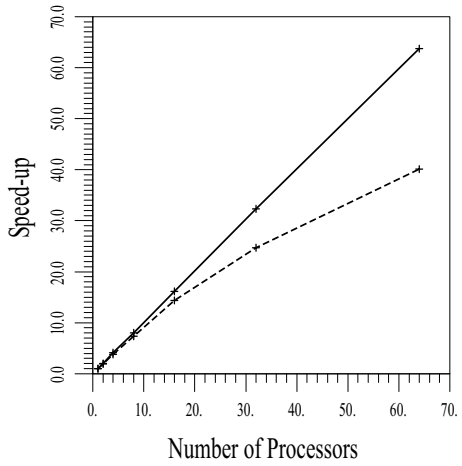

Fig. 9. Speed-up obtained parallelizing the outer loop (in continuous line) and the inner loop (in discontinuous line)

So our target code is the nesteed DO loops that compute the elemental matrices. We can parallelize the outer loop or the inner one. This is the first alternative to be studied. Figure 9 shows the evolution of the speed-up factor obtained with different number of processors for both types of parallelization in the analysis of the Barberá grounding system with a two-layer soil model (the speed-up factor has been referenced to the sequential CPU time). These results [11] have been obtained with the schedule option "Dynamic,1" (we will discuss the schedule options below), and the strict value is approximated by taking the minimum of 4 CPU time measures made for the same option (the variance of the four ones is very small, anyway). In some cases, we have obtained speed-ups bigger than the number of processors due to small errors in the measurement of CPU time by the processors, and to the additional optimization of the code that the parallel compiler introduces. Results are better when the outer loop is parallelized because the granularity is bigger in that way, and so the cost of managing the parallel execution is minor: since the numerical approach leads to a symmetric formulation, the

coupling of every element of the grid with each one of the others can be represented by a triangle of m columns, of which the first one has m rows and the last one has 1 row. Hence, if the outer loop is parallelized, the columns of the triangle, that is, the cycles of the outer loop, are distributed among the processors. Whereas, if the inner loop is parallelized, the rows of one column are distributed among the processors. In this case, when computations on that column are finished the program moves sequentially to the next one, where another distribution of its rows among the processors is performed. This effect of granularity is, of course, more sensible when the number of processors grows, as it can be seen in figure 9.

So we have shown that the parallelization of the outer loop is more profitable than the parallelization of the inner one. The cycles in this case will be the columns of that triangle that coples one element to the other ones. The way to distribute these cycles (that have very different sizes) among the processors becomes a decisive question.

Studying the speed-up factors (referenced to the sequential CPU time) obtained for the outer-loop parallelization with different number of processors by using different "schedule" OpenMP options results as follows[11]. Since the size of the cycles is linearly decreasing, "static" schedules with a high "chunk" (i.e., the number of cycles in a task) are the less profitable ones. When no chunk value is specified, all the columns are uniformly distributed in the beginning. "Dynamic" schedules improve this behaviour because as each processor finishes a task, it dynamically takes the next one. Best results are obtained for a dynamic schedule with a chunk parameter of 1 column. This is the most lively scheme, since there are never waiting processors, although it requires the biggest amount of parallelization management. "Guided" schedules distribute initially all the columns among all the processors into pieces with size exponentially varying. In this case, results are very similar to those obtained with the "dynamic" ones. In general, for any schedule, we obtained worse results when the chunk parameter and the number of processors are high because then some processors do not get any work.

Summarizing, speed-up factors obtained for the outer parallelization are very close to the number of processors for good schedules, that is, "dynamic" or "guided" with low chunk parameters. In the example, the Barberá grounding analysis in a two layer soil model, 99.9% of the work of the whole processing program is dealt with only 408 tasks; so we can ensure that the parallelization of this loop is very profitable.

6 Conclusions

In this paper we have presented a generalization of the Boundary Element numerical approach developed by the authors for grounding grids embedded in stratified soils. The proposed approach has been applied to the earthing analysis with different soil models by using the geometry and characteristics of a real grounding system. The layered models allow to analyze the influence of the variations in the soil conductivity with depth and in the surroundings of the grounding system.

As expected, the suitable selection of a soil model is a key point in grounding analysis.

We have demonstrated it is possible to obtain highly accurate results with the proposed boundary element numerical approach, and these results can be noticeably different depending on the type of soil model considered in the study. Consequently, since the grounding safety parameters may significantly change, it could be advisable to use the multi-layer soil formulation as a general rule in spite of the increase in the computational cost. We have shown that this computing effort can be strongly reduced with a suitable parallelization of the programming codes, obtaining very affordable total CPU times.

Acknowledgements

This work has been partially supported by the "Ministerio de Ciencia y Tecnología (project #1FD97-0108)" of the Spanish Government, cofinanced with European Union FEDER funds, by the power company "Unión Fenosa Ingeniería S.A.", and by research fellowships of the "European Center for Parallelism of Barcelona, CEPBA", the "Xunta de Galicia" and the "Universidad de La Coruña".

References

[1] IEEE Std.80, *IEEE Guide for safety in AC substation grounding*, New York, 2000.

[2] Sverak J.G., *Progress in Step and Touch Voltage Equations of ANSI/IEEE Std.80*, IEEE Transactions on Power Delivery,**13**, 762–767, 1999.

[3] Garret D.L., Pruitt J.G., *Problems Encountered with the APM of Analyzing Grounding Systems*, IEEE Transactions on Power Delivery,**104**, 4006–4023, 1985.

[4] Navarrina F., Colominas I., Casteleiro M., *Analytical Integration Techniques for Earthing Grid Computation by BEM*, In "Numerical Methods in Engineering and Applied Sciences", 1197–1206, CIMNE, Barcelona, 1992.

[5] Colominas I., Navarrina F., Casteleiro M., *A boundary element numerical approach for grounding grid computation*, Computer Methods and Applied Mechanics in Engineering, **174**, 73-90, 1999.

[6] M. Casteleiro, L.A. Hernández, I. Colominas and F. Navarrina, *Memory and User guide of system TOTBEM for CAD of grounding grids in electrical installations*, Civil Engineering School, Universidad de La Coruña, 1994.

[7] I. Colominas, F. Navarrina, M. Casteleiro, *A Boundary Element Formulation for the Substation Grounding Design*, Advances in Engineering Software, **30**, 603–700, 1999.

[8] Colominas I., Navarrina F., Casteleiro M., *A Numerical Formulation for Grounding Analysis in Stratified Soils*, Submitted to IEEE Transactions on Power Delivery, 1999.

[9] G.F. Tagg, *Earth Resistances*, Pitman, New York, 1964.

[10] Johnson C., *Numerical Solution of Partial Differential Equations by the Finite Element Method*, Cambridge Univ. Press, Cambridge, USA, 1987.

[11] J.Gómez-Calviño, I.Colominas, F.Navarrina, M.Casteleiro, J.M.Cela, *Parallel computing aided design of earthing systems for electrical substations in non homogeneous soil models*, In "Proceedings of the ICCP Workshops", 381—388; IEEE Computer Society Press, USA, 2000.